MPP-2004-33
CERN-PH-TH/2004-072
hep-ph/0511021

Flavour changing effects on $e^+e^- \to Hb\bar{s}$, $H\bar{b}s$ in the MSSM

W. Hollik[1], S. Peñaranda[2] and M. Vogt[1] *

[1] *Max-Planck-Institut für Physik, Föhringer Ring 6, D–80805 Munich, Germany*
[2] *CERN-TH Division, Department of Physics, CH-1211 Geneva 23, Switzerland*

Abstract

Flavour changing effects originating from the exchange of scalar particles in the processes $e^+e^- \to H^x b\bar{s}$, $H^x\bar{b}s$, with $H^x \equiv h^0, H^0, A^0$, are investigated in the Minimal Supersymmetric Standard Model with non-minimal flavour violation at the one-loop level. The dominating SUSY-QCD contributions with squark–gluino loops are calculated and discussed. We consider the SUSY scenario with non-minimal flavour mixing in the down-type squark-mass matrix. The flavour-changing cross sections are derived, and we discuss the dependence on the MSSM parameters and the strength of flavour mixing. The values for the cross section can reach 10^{-4} pb for the production of the heavy Higgs boson H^0 or A^0, and only 10^{-7} pb for the light Higgs boson h^0. Non-decoupling behaviour occurs for both h^0, H^0 production in the case of a common heavy SUSY mass scale.

*electronic addresses:
hollik@mppmu.mpg.de,
siannah.penaranda@cern.ch,
mvogt@mppmu.mpg.de

1 Introduction

Searching for Flavour Changing Neutral Currents (FCNC) is among the important tasks of the coming generation of high energy colliders [1]. FCNC processes are forbidden in the Standard Model (SM) at lowest order. These effects appear at the loop level and are of basic importance for testing the quantum structure of the SM. In the SM, however, the one-loop effects are small, suppressed by the GIM mechanism [2]. In models beyond the SM new non-standard particles appear in the loops, with significant contributions to flavour changing transitions [3]. Therefore, FCNC processes play an important role in searching new physics beyond the SM.

Among various new physics models, supersymmetry (SUSY), especially the Minimal Supersymmetric Standard Model (MSSM), is a favoured candidate [4]. The MSSM introduces two Higgs doublets to break the electroweak symmetry. After symmetry breaking, there are five physical Higgs bosons: two CP-even Higgs bosons ($h^0\,, H^0$), one CP-odd boson (A^0) and two charged Higgs bosons ($H^\pm$) [5]. The couplings of these Higgs particles may differ significantly from those of the SM. In fact, an important feature of SUSY models is that the fermion-Higgs couplings are no longer strictly proportional to the corresponding mass, as they are in the SM. In particular, the b-quark coupling to the neutral Higgs boson becomes enhanced for large $\tan\beta = v_2/v_1$, the ratio of the two vacuum expectation values [5] [1]. Since there are five Higgs bosons in the MSSM, additional features not present in the SM may be useful to pin down differences between those models, manifested in different coupling strengths, decay widths and production cross sections. In the minimal flavour violation scenario (MFV), the only source of flavour violation is mediated by the CKM-Matrix [3]. In the general MSSM with non-minimal flavour violation (NMFV), new flavour changing (FC) effects emerge due to a possible misalignment between the squark and the quark sector. The FC interactions resulting from such a misalignment do not show up at the tree-level, but they can be generated at the one-loop level and could lead to relevant contributions to observables for specific regions of the MSSM parameters. The MSSM with NMFV is considered in this paper.

The FCNC vertices in the SM and beyond have been extensively examined in the literature, and the results promise FCNC to provide a fertile ground for testing the SM and probing new physics. These analysis include rare decays of B-meson systems [6,7], Z-boson decays [8–10], and top decays [11]. It is known that the SM predictions for the top quark FCNC processes are far below the detectable level and that the MSSM can enhance them by several orders, making them potentially accessible at future collider experiments [12]. In particular, the branching ratios for $Z \to b\bar{s}$ decays are of the order of 10^{-8} in the SM [8], of the same order in SUSY with $\tilde{t}$-$\tilde{c}$ mixing and can reach 10^{-6} in SUSY with $\tilde{b}$-$\tilde{s}$ mixing [9], both last rates being dominated by the SUSY radiative effects from squark-gluino loops. FC effects that can be induced by squark-gluino loops in Higgs-boson decays have been investigated as well, and $BR(H^x \to b\bar{s}) \sim 10^{-4} - 10^{-3}$ and $BR(H^x \to t\bar{c}) \sim 10^{-4}$ have been found for selected regions of the MSSM parameter space and the flavour mixing parameters

[1] Explicitly they are proportional to $1/\cos\beta$, and to $[-\sin\alpha\,, \cos\alpha, \sin\beta]$ for $[h^0\,, H^0\,, A^0]$ respectively.

in the MSSM squark-mass matrices [13,14]. The electroweak corrections are subdominant, at least one order of magnitude smaller than the SUSY-QCD ones, but can give interference effects [15]. The large rates found for the SUSY contributions to the Higgs partial decay widths into $b\bar{s}$ and $s\bar{b}$, as well as to the effective FC Higgs couplings to quarks, are indeed quite encouraging [13–19]. Furthermore, effects of non-minimal flavour violation on the MSSM Higgs boson masses and the electroweak precision observables, m_W and $\sin\theta_{eff}$, has been investigated in [20].

FC effects in the SM in electron–positron collisions have been under study in several papers. In particular, the cross sections of $e^+e^- \to t\bar{c}$ and $e^+e^- \to b\bar{s}$ processes in the SM are analyzed in [21]. The cross section of the process with a $b\bar{s}$ final state was found to be larger than the one with a $t\bar{c}$ final state, but only of the order of 10^{-3} fb, which is too small to be observed at present and future colliders.

In this paper we investigate FC effects via associated bottom-strange and Higgs boson production in the MSSM. More concretely, we study the effects of squark-gluino loops in the higher-order processes

$$e^+e^- \to H^x b\bar{s} + H^x \bar{b}s \qquad (H^x \equiv h^0\,, H^0\,, A^0)\,, \tag{1.1}$$

and discuss the size of the induced cross sections at the one-loop level, with virtual second and third generation squarks, and their dependence on the MSSM parameters and the flavour mixing strength.

The paper is organized as follows: In section 2 we present a brief outline on squark mixing in the MSSM with NMFV. Section 3 gives an overview over the various classes of squark–gluino diagrams at the one-loop level and their impact on the total cross section, including both resonant diagrams (subsection 3.2) and non-resonant contributions (subsection 3.3). We discuss the dependence on the MSSM parameters in section 4. Additionally, the non-decoupling behaviour of the SUSY contributions in the large sparticle-mass limit is presented in section 5, and a summary is given in section 6.

2 Non-minimal squark mixing

Flavour changing phenomena in SUSY models can emanate from a mixing between different generations of squarks through the soft breaking terms in the Lagrangian of the squark sector. This non-minimal flavour mixing scenario, where squark mixing results from a misalignment between the quark and the squark mass matrices, is the most general case of the MSSM. We assume that the flavour changing squark mixing is significant only in transitions between third and second generation squarks. It is known that there are strong experimental bounds on the squark mixing involving the first generation, resulting from data on $K^0 - \bar{K}^0$ and $D^0 - \bar{D}^0$ mixing [3].

In general, the flavour violating quantities arise from non-diagonal entries in the bilinear soft breaking matrices $M^2_{\tilde{Q}}\,, M^2_{\tilde{U}}$ and $M^2_{\tilde{D}}$, that appear in the mass matrices in the up-squark and down-squark sectors as well as from non-diagonal (flavour changing) entries in the trilinear soft breaking matrices A_u and A_d. In our analysis, FC effects are generated

by the one-loop exchange of $\tilde{b}$-$\tilde{s}$-admixture states and gluinos, $\tilde{g}$. When the squark mass matrix is diagonalized, FC gluino-quark-squark couplings can be derived for the mass eigenstates and FC effects via squark-gluino loops are induced. It is known that some of the flavour mixing parameters in the $\tilde{b} - \tilde{s}$ sector are severely constrained by the $b \to s\gamma$ decays [3, 17, 22, 23], but in particular the ones referring to the LL- and RR-mixing of the SUSY partners of the left-handed and right-handed quarks, respectively, are not definitely excluded [3].

We assume the simplest case of mixing, where the only non-zero off-diagonal squark squared mass entries in the squark-sector stand for $\tilde{s}_L\tilde{b}_L$ and $\tilde{c}_L\tilde{t}_L$ mixing. Expressing the squark mass matrix in terms of the chirality eigenstates $\{s_L, s_R, b_L, b_R\}$ and $\{c_L, c_R, t_L, t_R\}$, respectively, and considering only LL-Mixing, i.e. mixing between the left-chiral components of the squarks leads to the following mass matrix mediating between the chiral eigenstates and the down-squark admixtures [13, 15],

$$M^2_{\tilde{u}} = \begin{pmatrix} M^2_{L,c} & m_c X_c & \lambda_{LL} M_{L,c} M_{L,t} & 0 \\ m_c X_c & M^2_{R,c} & 0 & 0 \\ \lambda_{LL} M_{L,c} M_{L,t} & 0 & M^2_{L,t} & m_t X_t \\ 0 & 0 & m_t X_t & M^2_{R,t} \end{pmatrix}, \tag{2.1}$$

$$M^2_{\tilde{d}} = \begin{pmatrix} M^2_{L,s} & m_s X_s & \lambda_{LL} M_{L,s} M_{L,b} & 0 \\ m_s X_s & M^2_{R,s} & 0 & 0 \\ \lambda_{LL} M_{L,s} M_{L,b} & 0 & M^2_{L,b} & m_b X_b \\ 0 & 0 & m_b X_b & M^2_{R,b} \end{pmatrix} \tag{2.2}$$

with

$$\begin{aligned} M^2_{L,q} &= M^2_{\tilde{Q},q} + m^2_q + \cos 2\beta (T^q_3 - Q_q s^2_W) m^2_Z \,, \\ M^2_{R,(c,t)} &= M^2_{\tilde{U},(c,t)} + m^2_{c,t} + \cos 2\beta Q_t s^2_W m^2_Z \,, \\ M^2_{R,(s,b)} &= M^2_{\tilde{D},(s,b)} + m^2_{s,b} + \cos 2\beta Q_b s^2_W m^2_Z \,, \\ X_{c,t} &= A_{c,t} - \mu \cot\beta \,, \\ X_{s,b} &= A_{s,b} - \mu \tan\beta \,, \end{aligned} \tag{2.3}$$

where $M_{L,q}$, $M_{R,q}$ are the corresponding bilinear soft SUSY breaking entries and m_q the quark matrices with $q \in \{b, s, c, t\}$. T^q_3 is the third component of the weak isospin, Q_q denotes the charge of the corresponding quark. The trilinear soft SUSY breaking matrices A_q are assumed to be diagonal, with entries $A_{s,b}$. μ is the mass parameter of the Higgs boson sector and $\tan\beta$ is the ratio of the vacuum expectation values in this sector. m_Z is the Z boson mass, and $s_W = \sin\theta_W$ contains the electroweak mixing angle θ_W. $\lambda \equiv \lambda_{LL}$ denotes the parameter characterizing the flavour mixing strength in the mixing of the LL-components of the second and third generation squarks [2]. Thus, we have only one free parameter determining the strength of FC.

[2]The flavour mixing parameter λ can be identified with $(\delta_{LL})_{23}$ in the usual notation of the mass-insertion approximation [3].

3 The loop-induced cross sections

In this section we discuss the various contributions leading to the production of a Higgs boson associated with a flavor-nondiagonal quark pair, $b\bar{s}$ or $s\bar{b}$. As far as the final states with $b\bar{s}$ and $s\bar{b}$ are experimentally not distinguished, the result for $\sigma(e^+e^- \to H^x\, b\,\bar{s} + H^x\, s\,\bar{b})$ is obtained by summing the two individual cross sections.

We have done the computation using *FeynArts*, *FeynCalc* and *FormCalc* [24]. Feynman rules of MSSM vertices with FC effects are recently implemented in *FeynArts* (extending the previous MSSM model file). The Higgs boson masses, the Higgs boson decays and the masses of the MSSM-spectrum have been computed using the *FeynHiggs2.1beta* Fortran code [25], including all FC effects. As the MSSM Higgs boson couplings to down-type fermions receive large quantum corrections enhanced by $\tan\beta$, these corrections have to be resummed to all orders in perturbation theory with the help of the effective Lagrangian formalism [26]. These leading threshold corrections to the bottom mass are taken into account in our computation in terms of the resummed version.

3.1 Kinematics

The cross section for the production process

$$e^-(p_a) + e^+(p_b) \to\ b(p_1) + \bar{s}(p_2) + H^x(p_3) \tag{3.1}$$

is given by the expression (neglecting the electron mass)

$$\sigma = \frac{1}{2s(2\pi)^5} \int \prod_{i=1}^{3} \left[\frac{\mathrm{d}^3 p_i}{2p_i^0}\right] \delta^4(p_a + p_b - \sum_i p_i)\, \overline{|\mathcal{M}|^2}\,, \tag{3.2}$$

involving an integration over the 5-dimensional phase space and $\overline{|\mathcal{M}|^2}$, the spin-averaged matrix-element squared of the process. The phase space integral can be expressed in terms of two energy and two angular variables, chosen in the overall CMS with $s = (p_a + p_b)^2$,

$$\sigma = \frac{1}{16s(2\pi)^4} \int_{m_1}^{p_1^+} \mathrm{d}p_1^0 \int_{p_2^-}^{p_2^+} \mathrm{d}p_2^0 \int_{-1}^{+1} \mathrm{d}\cos\theta \int_0^{2\pi} \mathrm{d}\eta\ \overline{|\mathcal{M}|^2}\,, \tag{3.3}$$

with the boundaries

$$\begin{aligned} p_1^+ &= \frac{\sqrt{s}}{2} - \frac{(m_2+m_3)^2 - m_1^2}{2\sqrt{s}}\,, \\ p_2^\pm &= \frac{1}{2\tau}\left[\sigma(\tau + m_+ m_-) \pm |\vec{p}_1|\sqrt{(\tau - m_+^2)(\tau - m_-^2)}\right], \end{aligned} \tag{3.4}$$

where

$$\sigma = \sqrt{s} - p_1^0,\ \tau = \sigma^2 - |\vec{p}_1|^2,\ m_\pm = m_2 \pm m_3\,.$$

θ is the angle between the momenta $\vec{p}_a$ and $\vec{p}_1$, and η the angle between the two planes spanned by $\vec{p}_1, \vec{p}_2$ and $\vec{p}_1, \vec{p}_a$.

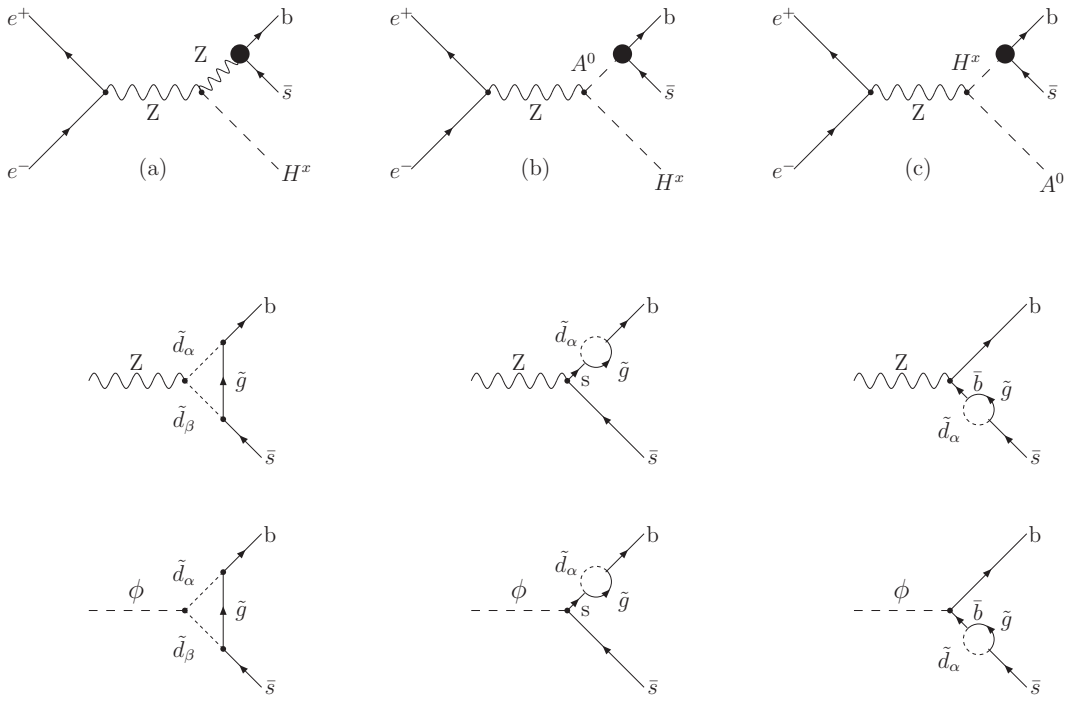

Figure 1: (a), (b), (c) Generic diagrams for resonant contributions to $\sigma(e^+e^- \to \phi\, b\, \bar{s} + \phi\, s\, \bar{b})$ ($\phi \equiv h^0, H^0, A^0$). (d) Gluino-squark loop contributions to $Z \to b\,\bar{s}$ and $\phi \to b\,\bar{s}$.

3.2 Resonant contributions

Due to the structure of the couplings of Higgs bosons to another Higgs boson and/or to a Z-boson in the MSSM, the $q\bar{q}H$ production processes receive large resonating contributions not present in the SM. The associated Higgs boson production with a heavy quark pair, $t\bar{t}$ and $b\bar{b}$, in e^+e^- collisions at high energy have been investigated and large resonant contributions that imply rates of a few fb have been found [27] for the $b\bar{b}$-pair. Here we consider the resonating contributions to the associated Higgs boson production with a quark pair $b\bar{s}$ in e^+e^- collisions.

The structure of the corresponding Feynman diagrams is shown in Fig. 1; other diagrams are suppressed by the small electron mass. In the kinematically allowed regions there are two types of resonating intermediate states for $H^x = h^0, H^0$ production, involving Z and A^0 resonances, $e^+e^- \to ZH^x$ with $Z \to b\bar{s}$, and $e^+e^- \to A^0H^x$ with $A^0 \to b\bar{s}$ (Fig. 1(a,b)). There are other resonances channels for A^0 production, involving h^0 and H^0 resonances; namely $e^+e^- \to A^0H^x$ with $H^x \to b\bar{s}$ (Fig. 1(c)). The result for the $H^x = h^0$ case (h^0 resonance) is several orders of magnitude smaller than the H^0 resonance case (see below), therefore we do not include this case in the discussion. These processes are

sensitive to the MSSM couplings of the Z boson to the Higgs boson H^x and to the $A^0 H^x$ pair, normalized to the standard ZZh_{SM} coupling given by

$$\begin{aligned} g_{ZA^0h^0} &= \cos(\beta-\alpha)\,, \quad g_{ZZh^0} = \sin(\beta-\alpha)\,, \\ g_{ZA^0H^0} &= \sin(\beta-\alpha)\,, \quad g_{ZZH^0} = \cos(\beta-\alpha)\,. \end{aligned} \tag{3.5}$$

For the computation, we treat the intermediate particle in the narrow-width approximation, i.e. multiplying the two-particle production cross section for on-shell particles with the corresponding branching ratios,

$$\begin{aligned} \sigma(e^+e^- \to H^x\, b\,\bar{s} + H^x\, s\,\bar{b}) &\simeq \sigma(e^+e^- \to H^x\, Z)\cdot BR(Z \to b\,\bar{s} + s\,\bar{b})\,, \\ \sigma(e^+e^- \to H^x\, b\,\bar{s} + H^x\, s\,\bar{b}) &\simeq \sigma(e^+e^- \to H^x\, A^0)\cdot BR(A^0 \to b\,\bar{s} + s\,\bar{b})\,, \\ \sigma(e^+e^- \to H^x\, b\,\bar{s} + H^x\, s\,\bar{b}) &\simeq \sigma(e^+e^- \to H^x\, A^0)\cdot BR(H^x \to b\,\bar{s} + s\,\bar{b})\,, \end{aligned} \tag{3.6}$$

which yields a good approximation owing to the small total decay widths of the intermediate resonances. The flavor-changing Z, A^0 and H^x decays are loop-induced, with the gluino-squark strong contributions shown in Fig. 1(d) as the dominating source, yielding the branching ratios of $Y = Z, A^0, H^x$,

$$BR\,(\,Y \to b\,\bar{s} + s\,\bar{b}\,) = \frac{\Gamma\,(\,Y \to b\,\bar{s}\,) + \Gamma\,(\,Y \to s\,\bar{b}\,)}{\Gamma_{\rm tot}(Y)}\,, \tag{3.7}$$

where $\Gamma_{\rm tot}(Y)$ is the total width in each case.

Although numerical results and a discussion of the parameter dependence will be given in the next section, we want to illustrate here the size of the various contributions, choosing $m_A = 250$ GeV, $\tan\beta = 35$, and the SUSY parameters of (4.1). For the value $\lambda = 0.6$ of the mixing parameter, one obtains the following branching ratios,

$$\begin{aligned} BR(A^0 \to b\,\bar{s} + s\,\bar{b}) &\sim 10^{-2}\,, \qquad BR(H^0 \to b\,\bar{s} + s\,\bar{b}) \sim 10^{-2}\,, \\ BR(h^0 \to b\,\bar{s} + s\,\bar{b}) &\sim 10^{-4}\,, \qquad BR(Z \to b\,\bar{s} + s\,\bar{b}) \sim 10^{-11}\,. \end{aligned} \tag{3.8}$$

Here the threshold corrections on the b-quark mass are considered. This implies that the results for $Z \to b\,\bar{s}$ are different from the ones given in [9]. For $m_b = 5$ GeV we can reproduce the previous results.

The couplings given in (3.5) can be suppressed if either $\sin(\beta-\alpha)$ or $\cos(\beta-\alpha)$ is very small. In particular for large $\tan\beta$ and not too low m_A, as it is the case for the choice of input parameters (4.1), the ZA^0h^0 and ZZH^0 couplings are suppressed and the couplings for ZA^0H^0 and ZZh^0 are large. Hence, the cross sections for $e^+e^- \to H^0\,A^0$ and $e^+e^- \to h^0\,Z$ are about 2–3 orders of magnitude larger than for $e^+e^- \to h^0\,A^0$ and $e^+e^- \to H^0\,Z$, at $\sqrt{s} = 500$ GeV amounting to

$$\begin{aligned} \sigma(e^+e^- \to H^0\,A^0) &\simeq 10^{-2}\,\text{pb}\,, \qquad \sigma(e^+e^- \to h^0\,Z) \simeq 10^{-2} - 10^{-1}\,\text{pb}, \\ \sigma(e^+e^- \to h^0\,A^0) &\simeq 10^{-5} - 10^{-4}\,\text{pb}\,, \qquad \sigma(e^+e^- \to H^0\,Z) \simeq 10^{-5} - 10^{-3}\text{pb}\,. \end{aligned} \tag{3.9}$$

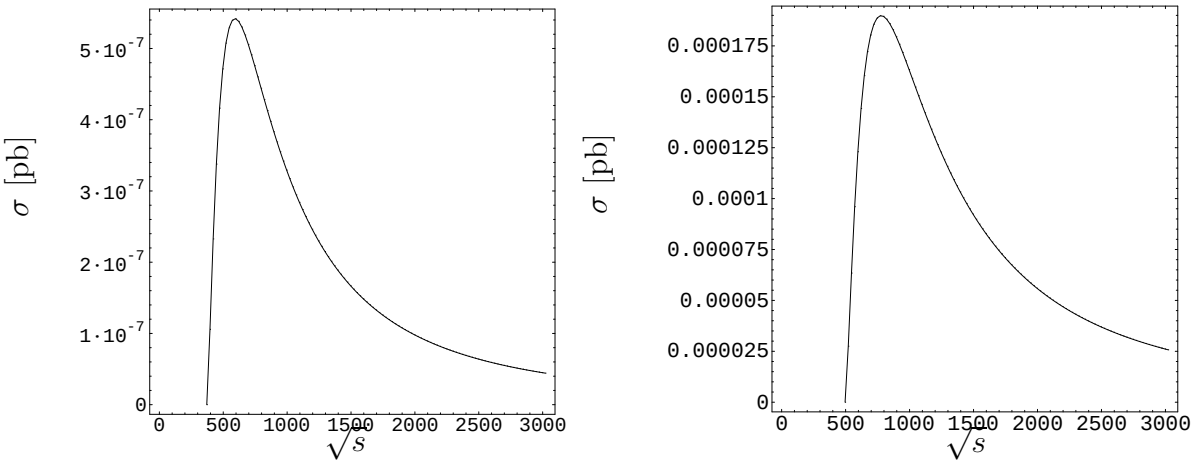

Figure 2: A^0-resonant contributions to $\sigma(e^+e^- \to H^x\, b\, \bar{s} + H^x\, s\, \bar{b})$ as a function of $\sqrt{s}$ [GeV] for $H^x \equiv h^0$ (left) and $H^x \equiv H^0$ (right), with $\lambda = 0.6$.

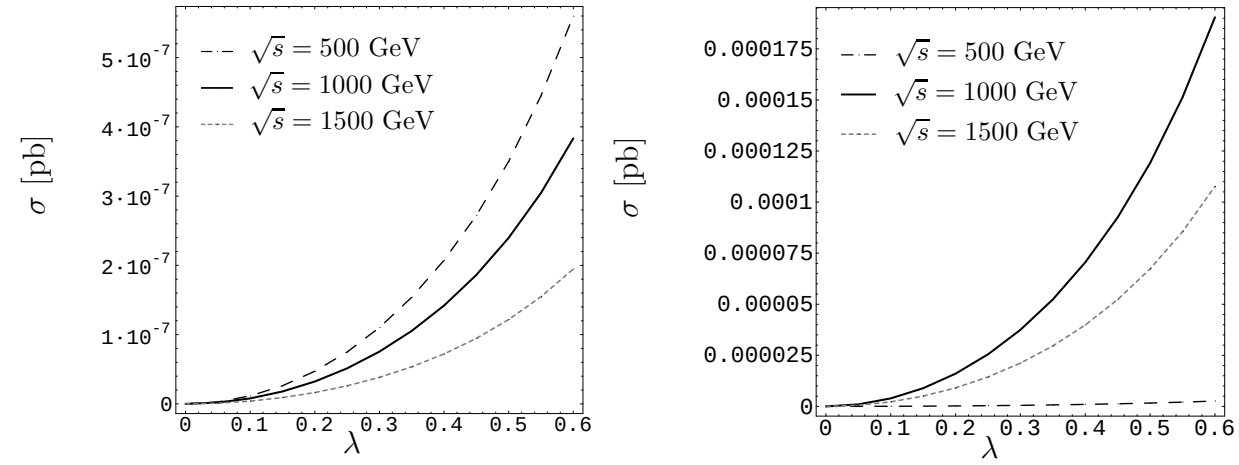

Figure 3: Resonant contributions to $\sigma(e^+e^- \to H^x\, b\, \bar{s} + H^x\, s\, \bar{b})$ as a function of λ at $\sqrt{s} = 500$ GeV, 1000 GeV, 1500 GeV, for h^0 (left), H^0 (right).

Therefore, we can conclude that the Z-resonance contribution for the $H^x b\bar{s}$ final state ($H^x \equiv h^0\,, H^0\,, A^0$) are very small, at most of the order of 10^{-12} pb, and the h^0-resonance contributions are of the order of 10^{-8} pb, whereas the contributions with heavy Higgs bosons ($A^0\,, H^0$) intermediate states can reach 10^{-4} pb for the cross section.

In Fig. 2 we show the behaviour of the cross section with the center of mass energy, based on the dominant contributions with the A^0 intermediate states, Fig. 1(b), for both h^0 (left panel) and H^0 (right panel). Since the results for the contributions with H^0 intermediate states, Fig. 1(c), are very similar, we do not include explicit numerical results for this case. The behaviour of the cross section with both the center of mass energy and the flavour parameter λ for the case of A^0 intermediate states are straightforwardly applied

to the H^0 case. If not stated differently, the value of λ is fixed to be $\lambda = 0.6$. The variation of the cross section with λ is contained in Fig. 3, shown for three different values of the energy, $\sqrt{s} = 500\,, 1000\,, 1500$ GeV. The effects increase with λ for both kind of Higgs bosons and vanish at $\lambda = 0$, as to be expected. In the H^0 case, due to kinematical reasons, the cross section at $\sqrt{s} = 500$ GeV is smaller than at 1 TeV, leading to an inversion of the order of the curves. In particular for the light Higgs boson h^0, the cross section remains rather small, although it is effectively for a two-particle process with subsequent decay. The resonating behaviour is largely canceled by either a small Zh^0A^0 coupling or a tiny branching ratio of the Z boson. Therefore, also non-resonant contributions have to be considered for a reliable estimate of the total production rate.

3.3 Non-resonant contributions

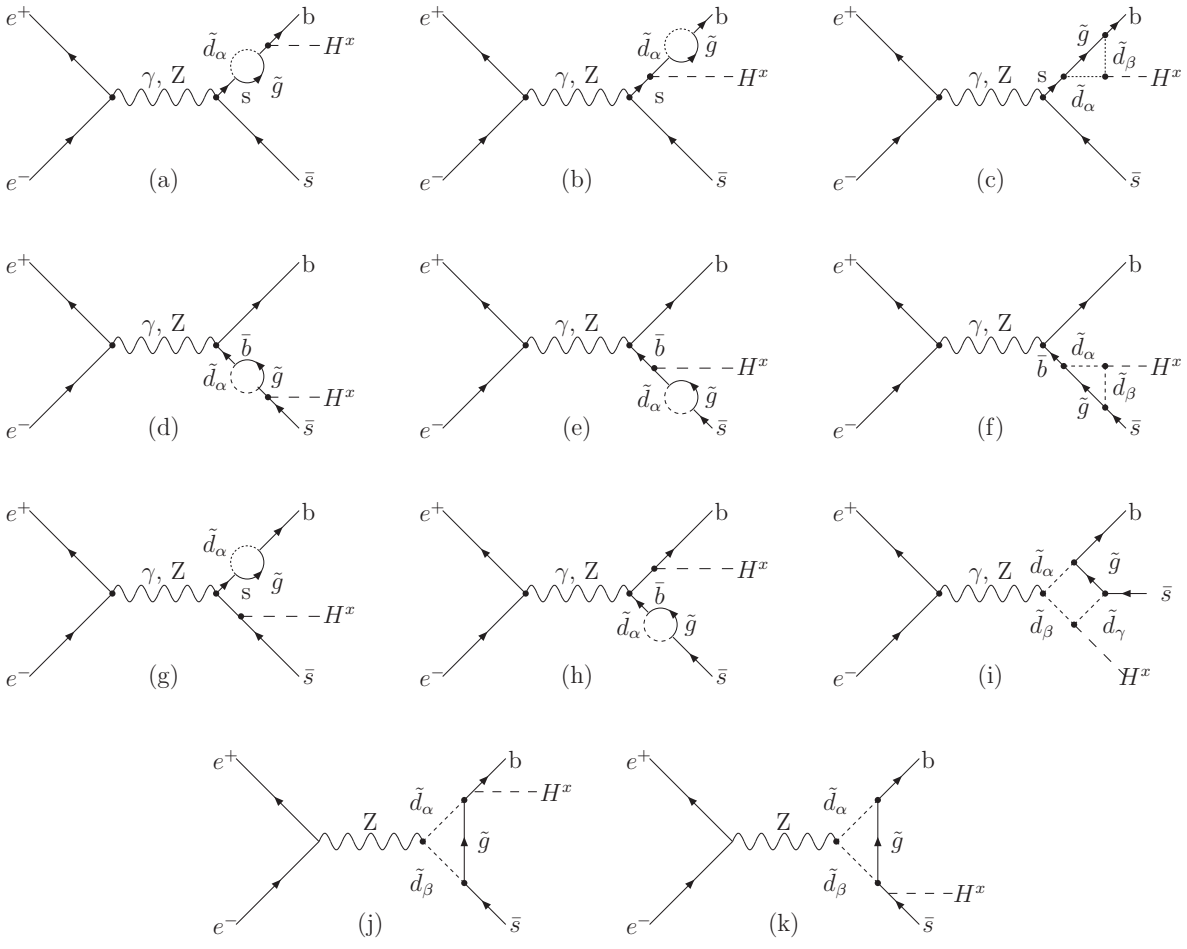

Figure 4: Generic diagrams for the squark-gluino one-loop contributions to $e^+e^- \to H^x\, b\, \bar{s} + H^x\, s\, \bar{b}$ ($H^x \equiv h^0\,, H^0\,, A^0$).

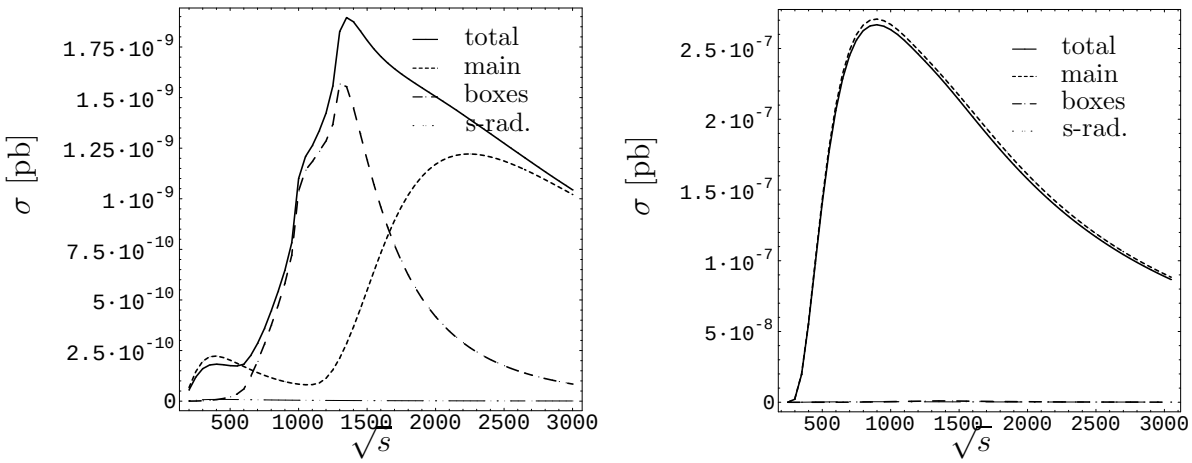

Figure 5: One-loop contributions to $\sigma(e^+e^- \to H^x\, b\, \bar{s} + H^x\, s\, \bar{b})$ as a function of $\sqrt{s}$ (GeV). Total cross sections, *main* and *box* contributions, and corrections with Higgs radiation off the s-lines ($h^0 \equiv$ left panel, $H^0 \equiv$ right panel). Here $\lambda = 0.6$.

Besides the two-particle-like processes discussed in the previous subsection, there are non-resonating contributions for $H^x b\bar{s}$ production, which are genuine $2 \to 3$ processes. The set of diagrams under consideration is shown in Fig. 4. There are three different types of relevant topologies: self-energy, triangle, and box diagrams. For the self-energy diagrams one has to distinguish between two different cases of Higgs radiation, one with radiation from b-lines and the other one with radiation from s-lines. Because of the small Yukawa couplings for the s case, only Higgs radiation from b-quarks will be of significance.

Here we outline the size of the contributions of each class of diagrams to the cross section for illustrational purposes, based on the same set of model parameters as in subsection 3.2. The non-resonant $e^+e^- \to Z \to bs$ contributions with Higgs radiation from b, s-lines (Fig. 4(j,k)) are suppressed with respect to the other contributions, being of the order of $10^{-12} - 10^{-14}$ pb, therefore they are not included in the analysis.

In Fig. 5 the one-loop contributions from the diagrams in Fig. 4 are depicted as a function of the center of mass energy $\sqrt{s}$. Since the results for $\sigma(e^+e^- \to H^0\, b\, \bar{s} + H^0\, s\, \bar{b})$ and $\sigma(e^+e^- \to A^0\, b\, \bar{s} + A^0\, s\, \bar{b})$ are very similar, we do not include explicit numerical results for A^0 production. The discussion for the H^0 case can straightforwardly be applied to the A^0 case along this paper. Besides the total cross sections (solid line) we list in addition the contributions from three different topologies independently: *main* contributions (short-dashed line), defined as the ones resulting from triangle diagrams and from self-energy diagrams with Higgs radiation off the b-lines, *box* contributions (long-dashed line), and the *s-rad* contributions, defined as the self-energy contributions with Higgs radiation off the s-lines. These last contributions are presented here for illustrational purposes, they are of the order of roughly 10^{-11} pb for both Higgs bosons. In the case of the heavy Higgs bosons, the box contributions are smaller than in the h^0 case, being of the order of $10^{-10} - 10^{-11}$ pb,

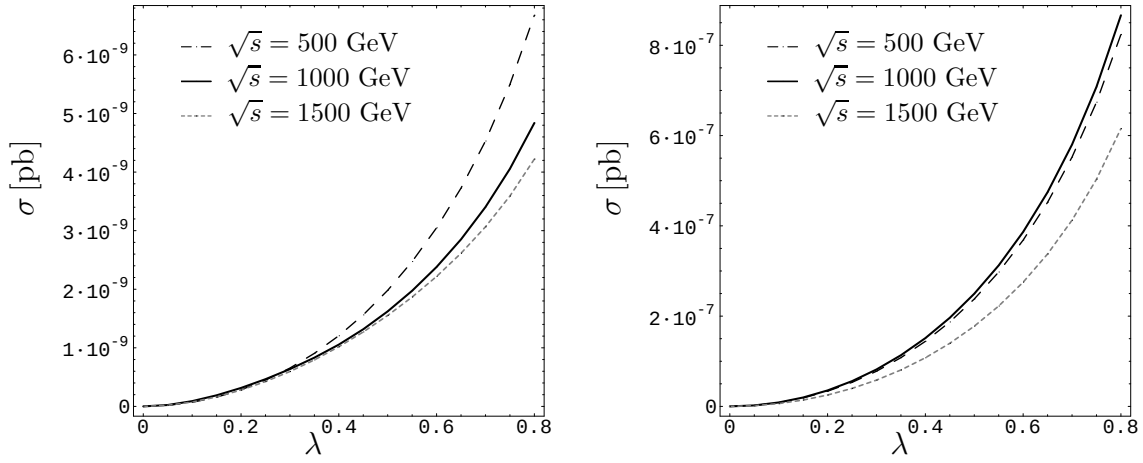

Figure 6: $e^+e^- \to H^x \to b\bar{s} + s\bar{b}$ cross section as a function of λ at $\sqrt{s} = 500\,,\, 1000\,,\, 1500$ GeV.

therefore they appear together with the contributions with Higgs radiation on the s-lines near to zero. For the case of h^0 production, there are several peaks corresponding to squark-mass thresholds in the loop integrals. These peaks are less distinctive in the H^0 case because they appear only in the box contributions, which are smaller for H^0.

One can see from Fig. 5 that for both Higgs bosons the non-resonant contributions are roughly two orders of magnitude smaller than the resonant contributions analyzed before. The dependence of the cross sections on the mixing parameter λ is illustrated in Fig. 6 at 1 TeV. As before, the cross sections increase with λ, being exactly zero for $\lambda = 0$.

4 Dependence on the MSSM parameters.

The SUSY parameter set needed to determine the input for $e^+e^- \to H^x\, b\,\bar{s} + H^x\, s\,\bar{b}$ ($H^x \equiv h^0, H^0$) consists of the quantities m_A, $\tan\beta$, μ, $M_{\tilde{g}}$, M_0, A, where M_0 is a common value for the soft-breaking squark mass parameters, $M_0 = M_{\tilde{Q},q} = M_{\tilde{U},(c,t)} = M_{\tilde{D},(s,b)}$, and A denotes the trilinear parameters which are chosen to be equal, $A_t = A_b = A_c = A_s = A$; $M_{\tilde{g}}$ is the mass of the gluino. These six parameters will be varied over a broad range, subject to the requirements that all the squark masses be heavier than 150 GeV [28] and $M_{h_0} > 114.4$ GeV [29]. Similarly, in view of the present experimental bounds on the chargino mass [28], we consider only $|\mu|$ values above 90 GeV. The flavour mixing parameter, λ, is constrained by the lower squark-mass bounds. For those parameters that are kept fixed in the various figures the following default set has been chosen,

$$\begin{aligned} \mu = 1000\,\mathrm{GeV}\,, M_0 = 500\,\mathrm{GeV}\,, A = 800\,\mathrm{GeV}\,, \\ m_A = 250\,\mathrm{GeV}\,, M_{\tilde{g}} = 800\,\mathrm{GeV}\,, \tan\beta = 35\,, \end{aligned} \tag{4.1}$$

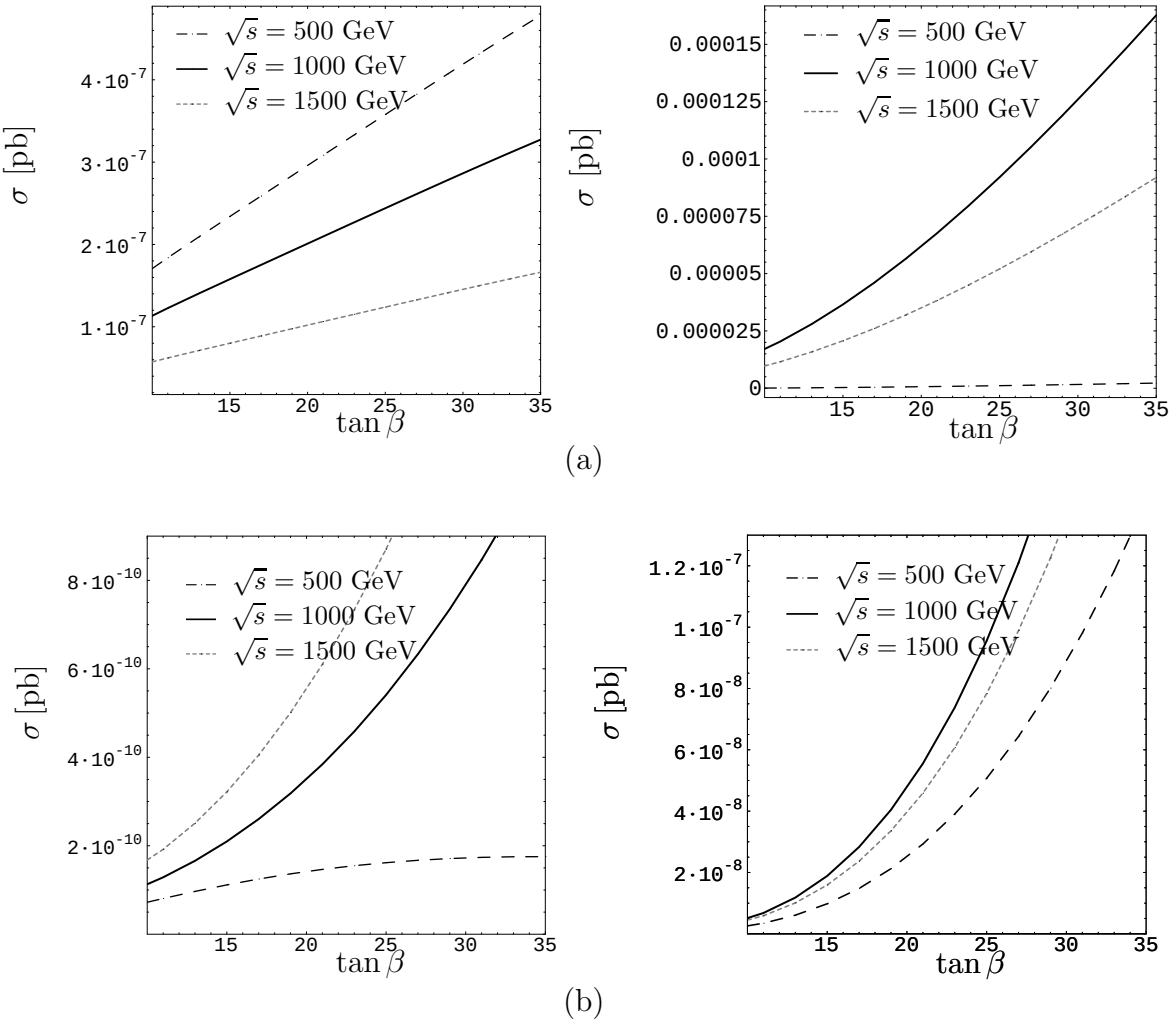

Figure 7: Cross section as a function of $\tan\beta$, at $\sqrt{s} = 500\,, 1000\,, 1500$ GeV for: **(a)** $e^+e^- \to A^0 H^x \to H^x\, b\,\bar{s} + H^x\, s\,\bar{b}$, **(b)** non-resonant $e^+e^- \to H^x\, b\,\bar{s} + H^x\, s\,\bar{b}$.

which is in accordance with experimental bounds for the decay $b \to s\gamma$ [30], as checked with the help of the code *micrOMEGAs* [31], based on minimal flavour violation calculations at leading order [32] and some contributions beyond leading order that are important for high values of $\tan\beta$ [33], as well as in accordance with the result for the muonic $(g-2)$. The FCNC effects in the rare decay $b \to s\gamma$ may impose severe constraints on MSSM parameters that reduce the maximally allowed value for $BR(h^0 \to b\,\bar{s})$ [14]. Furthermore, starting from (4.1), $\lambda > 0.8$ implies unallowed values for the squark masses, i.e. $M_{\tilde{q}} < 150$ GeV. If not stated differently, $\lambda = 0.6$ is a default value.

In the following we explore the dependence of the cross section on the MSSM parameters for both resonant and non-resonant diagrams, illustrated in Figs. 7 to Figs. 10; therein,

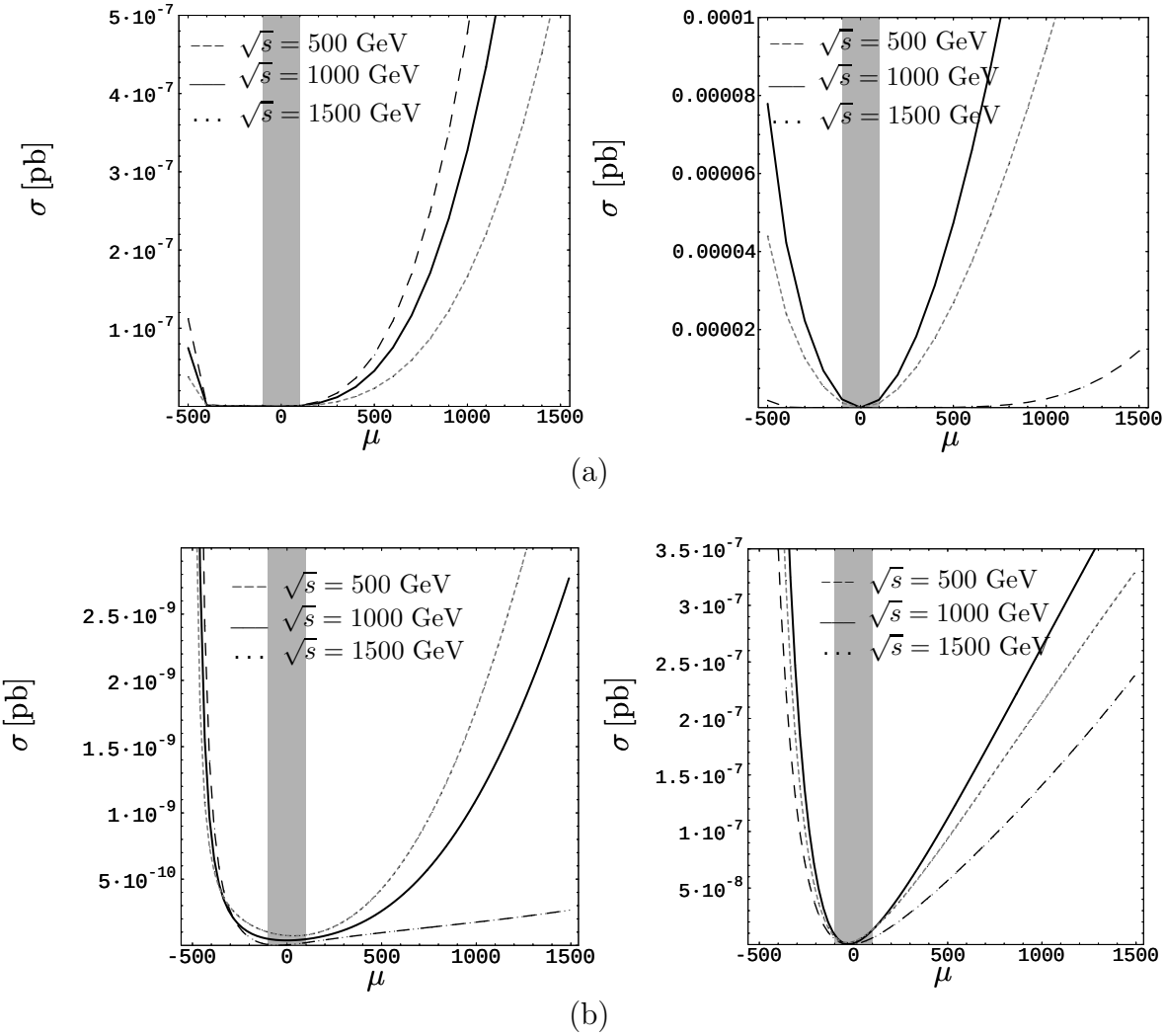

Figure 8: Cross section as a function as a function of μ (GeV) at $\sqrt{s} = 500\,, 1000\,, 1500$ GeV for: **(a)** $e^+e^- \to A^0 H^x \to H^x\, b\,\bar{s} + H^x\, s\,\bar{b}$, **(b)** non-resonant $e^+e^- \to H^x\, b\,\bar{s} + H^x\, s\,\bar{b}$.

the upper panels correspond to the resonant contributions and the lower panels show the non-resonant contributions.

First, we discuss the dependence on $\tan\beta$, the parameter that appears inside the couplings as well as in the squark-mass matrices and thus determines the squark-mass splitting and the b-mass corrections. Fig. 7 contains the cross section $\sigma(e^+e^- \to H^x\, b\,\bar{s} + H^x\, s\,\bar{b})$ versus $\tan\beta$ for three values of the center mass energy, $\sqrt{s} = 500\,, 1000\,, 1500$ GeV. In all cases, the cross sections increasing with $\tan\beta$. For the h^0 boson (left panel) the increase with $\tan\beta$ is slower due to a superposition of two different effects in the involved subprocesses: the reinforcement in the decay subprocess from the coupling enhancement is partly compensated by decreasing in $\cos(\beta - \alpha)$ in the production cross section of the

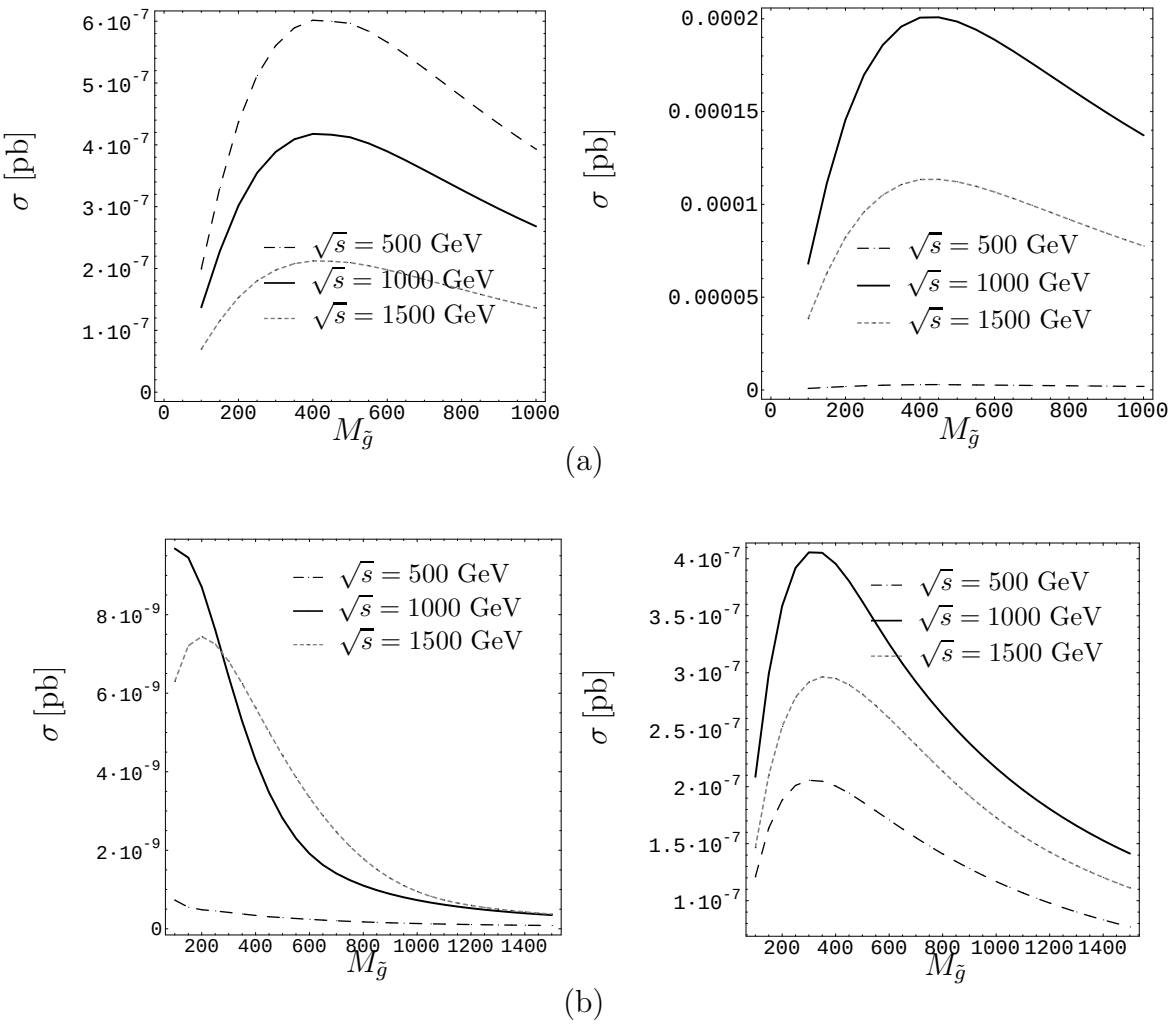

Figure 9: Cross section as a function of $M_{\tilde{g}}$ (GeV) at $\sqrt{s} = 500\,,\, 1000\,,\, 1500$ GeV for: **(a)** $e^+e^- \to A^0 H^x \to H^x\, b\, \bar{s} + H^x\, s\, \bar{b}$, **(b)** non-resonant $e^+e^- \to H^x\, b\, \bar{s} + H^x\, s\, \bar{b}$.

$2 \to 2$ process, which causes the almost linear shape of the $\tan\beta$ dependence. Values of $\tan\beta < 10$ are not included in these plots because they imply Higgs boson mass values lower than 114.4 GeV.

The dependence on the μ parameter for the h^0 (left) and H^0 case (right) is shown in Fig. 8. The shaded regions in these figures correspond to the regions excluded by the LEP bounds on the chargino mass, $|\mu| \leq 90$ GeV. One can see that in all cases the results for the cross sections are not symmetric under $\mu \to -\mu$. This is essentially due to the inclusion of the threshold corrections to the bottom quark mass, where the sign of μ plays an important role. We found that the corrections grow with the μ parameter.

Next we study the behaviour with respect to the other MSSM parameters. It turns out

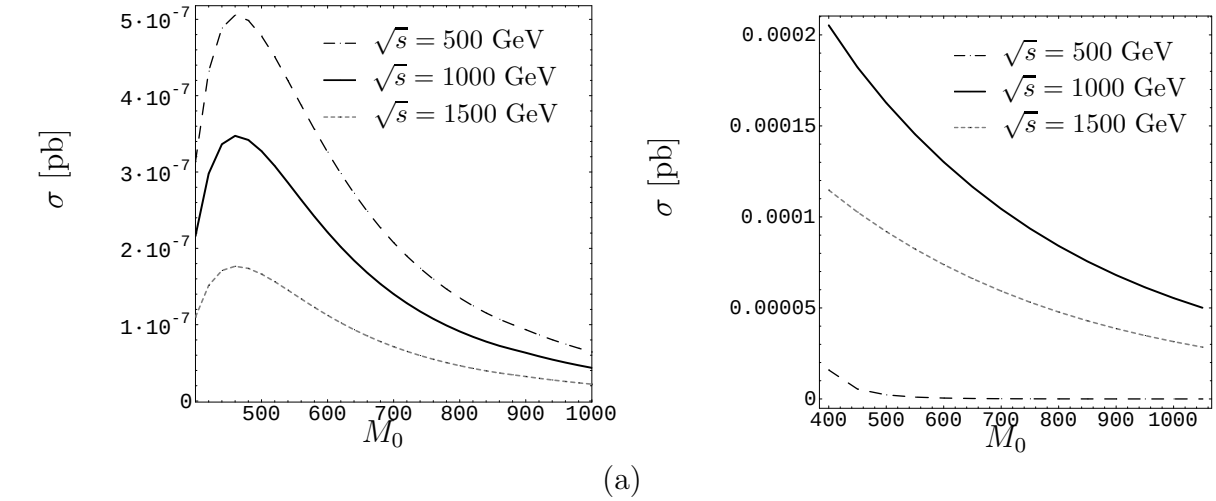

(a)

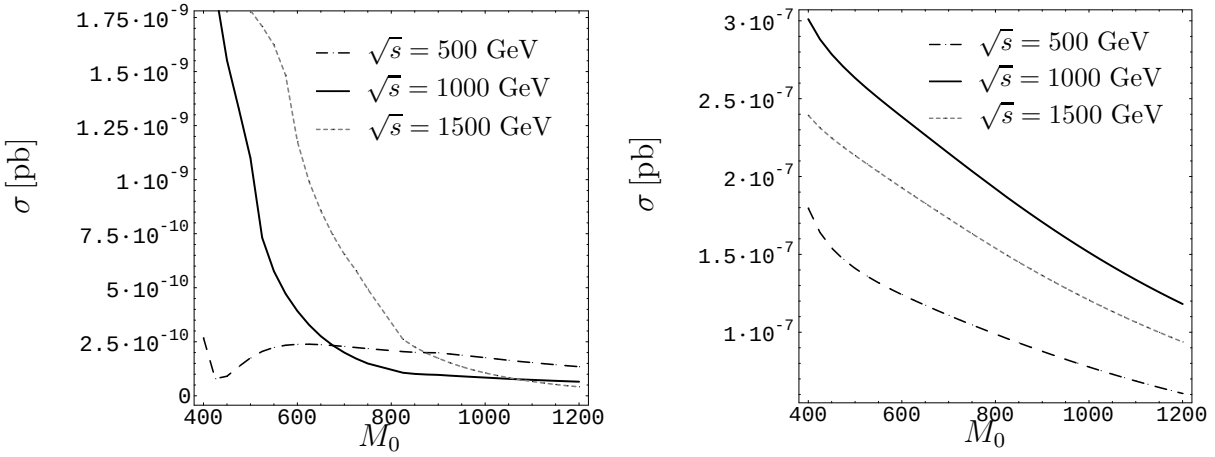

(b)

Figure 10: Cross section as a function of M_0 (GeV) at $\sqrt{s} = 500\,,\, 1000\,,\, 1500$ GeV for: **(a)** $e^+e^- \to A^0 H^x \to H^x\, b\, \bar{s} + H^x\, s\, \bar{b}$, **(b)** non-resonant $e^+e^- \to H^x\, b\, \bar{s} + H^x\, s\, \bar{b}$.

that the cross sections are nearly independent of the common trilinear parameters A. In Fig. 9 we show the dependence on the gluino mass, $M_{\tilde{g}}$. One can see from this figure that for all cases the FCNC effects vanish for heavy gluinos, i.e. the gluino decouples when only the gluino mass is varied. It is also interesting to see that the maximum is reached not for the smallest values but for intermediate values of the gluino mass.

The dependence of the cross sections on the common soft SUSY breaking squark mass parameter M_0 GeV is displayed in Fig. 10. Regions below $M_0 = 400$ GeV are not dropped because they would lead to excluded values for the down-squark masses. The FC cross

sections decrease with M_0, showing the independent decoupling behaviour of M_0.

In summary, the study of the dependence on the MSSM parameters, has confirmed the maximum size of the cross sections of the order of 10^{-7} pb for h^0 and $\mathcal{O}(10^{-4})$ pb for the H^0 case and demonstrates the individual decoupling behaviour of the virtual SUSY particles.

5 Non-decoupling behaviour of heavy SUSY particles

Here we analyze the non-decoupling behaviour of squarks and gluinos in SUSY-QCD contributions to our FCNC e^+e^- processes that result in a non-vanishing cross section also for very heavy SUSY particles. Non-decoupling behaviour of SUSY particles also occurs in the SUSY-QCD and SUSY-EW contributions to FCNC Higgs boson decays [13, 15].

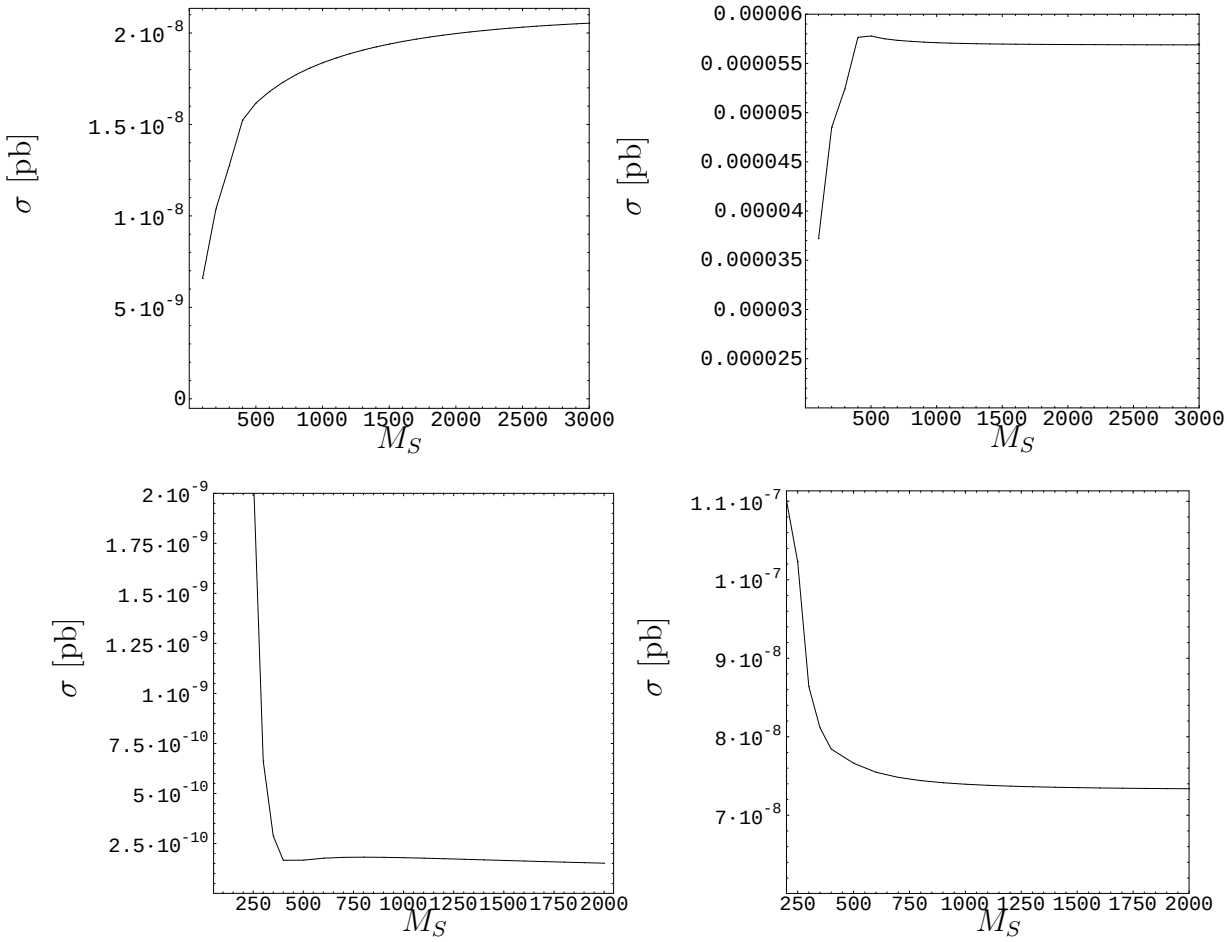

Figure 11: Non-decoupling behaviour of the cross section from resonant contributions (upper panels), and of $\sigma(e^+e^- \to H^x \to b\bar{s} + s\bar{b})$ from non-resonant contributions (lower panels). M_S, in GeV, is defined in (5.1).

In general, a non-decoupling behaviour originates from a compensation of the mass suppression induced through the heavy-particle propagators, by mass terms in the interaction vertices. Non-decoupling behaviour has previously been analyzed in detail in the case of flavour-preserving MSSM Higgs boson decays [34–37]. The non-decoupling contributions to effective FC Higgs Yukawa couplings have also been studied in the effective-Lagrangian approach for the quark sector [18, 19] and the lepton sector [38].

A condition for non-decoupling of SUSY particles is a common scale for all SUSY mass parameters. For the simplest assumption, the values of the SUSY masses, where all the soft breaking squark mass parameters, collectively denoted by M_0, the μ parameter, the trilinear parameters, collectively denoted by A, and the gluino mass $M_{\tilde{g}}$, are chosen to be of the same size and much larger than the electroweak scale M_{EW},

$$M_S \equiv M_0 = M_{\tilde{g}} = \mu = A \gg M_{EW}\,. \tag{5.1}$$

The numerical results of the analysis are shown in Fig. 11 for both h^0, H^0 production (for $\lambda = 0.6$). One can see that the cross sections tend to a non-vanishing value for large values of M_S, a behaviour characteristic of non-decoupling. While M_S is displayed only up to 2 or 3 TeV, we have checked that the cross sections remain stable even for very large values of M_S.

6 Conclusions

We have considered the production of neutral MSSM Higgs bosons in association with $b\bar{s}$ and $s\bar{b}$ quark pairs. We analyzed the flavour changing effects emanating from squark-gluino one-loop contributions, which are the dominant ones in a scenario with non-minimal flavor mixing in the squark sector. Both resonant contributions with an intermediate on-shell A^0 boson and non-resonant contributions have been investigated. The highest cross sections for $e^+e^- \to h^0 b\bar{s} + h^0 s\bar{b}$ are of $\mathcal{O}(10^{-7})$ pb and of $\mathcal{O}(10^{-4})$ pb for $e^+e^- \to H^0 b\bar{s} + H^0 s\bar{b}$ (and similar for A^0) which will be too low to be seen at a future linear collider.

One feature of the SUSY-QCD contributions of general basic interest is their non-decoupling behaviour for large values of the SUSY particle masses. The flavour changing cross sections, when all soft breaking mass parameters, μ and the trilinear parameters, are of the same order of magnitude and much larger than the electroweak scale, do not vanish but tend to a constant value.

Acknowledgments

This work was supported in part by the European Community's Human Potential Programme under contract HPRN-CT-2000-00149 "Physics at Colliders". We are grateful to T. Hahn, S. Dittmaier and S. Heinemeyer for computing assistance and useful discussions. We thank P. Slavich for many fruitful discussions and for reading the manuscript. Part of the work of S.P. has been supported by the European Union under contract No. MEIF-CT-2003-500030.

References

[1] Z. Zhao *et al.*, in *Proc. of the APS/DPF/DPB Summer Study on the Future of Particle Physics (Snowmass 2001)* ed. N. Graf, eConf **C010630** (2001) E2001 [hep-ex/0201047].

[2] S. L. Glashow, J. Iliopoulos and L. Maiani, Phys. Rev. **D2** (1970) 1285.

[3] F. Gabbiani and A. Masiero, Nucl. Phys. **B322** (1989) 235; F. Gabbiani, E. Gabrielli, A. Masiero and L. Silvestrini, Nucl. Phys. **B477** (1996) 321 [hep-ph/9604387]; M. Misiak, S. Pokorski and J. Rosiek, Adv. Ser. Direct. High Energy Phys. **15** (1998) 795 [hep-ph/9703442].

[4] H. P. Nilles, Phys. Rept. **110** (1984) 1; H. E. Haber and G. L. Kane, Phys. Rept. **117** (1985) 75.

[5] J. F. Gunion, H. E. Haber, G. L. Kane and S. Dawson, *"The Higgs Hunter's Guide"*, SCIPP-89/13, Addison-Wesley, Menlo-Park, 1990.

[6] C. S. Huang, W. Liao and Q. S. Yan, Phys. Rev. **D59** (1999) 011701, [hep-ph/9803460]; C. S. Huang, W. Liao, Q. S. Yan and S. H. Zhu, Phys. Rev. **D63** (2001) 114021 [Erratum-ibid. **D64** (2001) 059902] [hep-ph/0006250]; J. Cao, Z. H. Xiong and J. M. Yang, Nucl. Phys. **B651** (2003) 87 [hep-ph/0208035].

[7] A. J. Buras, hep-ph/0101336, hep-ph/9806471; A. J. Buras, P. H. Chankowski, J. Rosiek and L. Slawianowska, Nucl. Phys. **B659** (2003) 3 [hep-ph/0210145]; Phys. Lett. **B546** (2002) 96 [hep-ph/0207241].

[8] M. Clements, C. Footman, A. Kronfeld, S. Narasimhan and D. Photiadis, Phys. Rev. **D27** (1983) 570; W. S. Hou, N. G. Deshpande, G. Eilam and A. Soni, Phys. Rev. Lett. **57** (1986) 1406; J. Bernabeu, M. B. Gavela and A. Santamaria, Phys. Rev. Lett. **57** (1986) 1514.

[9] D. Atwood, S. Bar-Shalom, G. Eilam and A. Soni, Phys. Rev. **D66** (2002) 093005 [hep-ph/0203200].

[10] B. Mukhopadhyaya and A. Raychaudhuri, Phys. Rev. **D39**, 280 (1989); F. Gabbiani, J. H. Kim and A. Masiero, Phys. Lett. **B214** (1988) 398; W. S. Hou and R. G. Stuart, Phys. Lett. **B226** (1989) 122; B. Grzadkowski, J. F. Gunion and P. Krawczyk, Phys. Lett. **B268** (1991) 106.

[11] J. Guasch and J. Sola, Nucl. Phys. **B562** (1999) 3 [hep-ph/9906268] and references therein; S. Bejar, J. Guasch and J. Sola, Nucl. Phys. **B600** (2001) 21 [hep-ph/0011091]; Nucl. Phys. **B675** (2003) 270 [hep-ph/0307144]; J. J. Liu, C. S. Li, L. L. Yang and L. G. Jin, Phys. Lett. B **599** (2004) 92 [hep-ph/0406155].

[12] J. A. Aguilar-Saavedra and G. C. Branco, Phys. Lett. **B495** (2000) 347 [hep-ph/0004190]; J. A. Aguilar-Saavedra, Phys. Lett. **B502** (2001) 115 [hep-ph/0012305]; J. A. Aguilar-Saavedra and T. Riemann, hep-ph/0102197.

[13] A. M. Curiel, M. J. Herrero and D. Temes, Phys. Rev. **D67** (2003) 075008 [hep-ph/0210335].

[14] S. Bejar, F. Dilme, J. Guasch and J. Sola, JHEP **0408** (2004) 018 [hep-ph/0402188]; S. Bejar, J. Guasch and J. Sola, JHEP **0510** (2005) 113 [hep-ph/0508043].

[15] A. M. Curiel, M. J. Herrero, W. Hollik, F. Merz and S. Peñaranda, Phys. Rev. **D69** (2004) 075009 [hep-ph/0312135].

[16] K. S. Babu and C. F. Kolda, Rev. Lett. **84**, 228 (2000) [hep-ph/9909476]; P. H. Chankowski and L. Slawianowska, Phys.Rev. **D63**, 054012 (2001) [hep-ph/0008046]; C. Bobeth, T. Ewerth, F. Kruger and J. Urban, Phys.Rev. **D64**, 074014 (2001) [hep-ph/0104284]; Phys.Rev. **D66** 074021 (2002) [hep-ph/0204225].

[17] G. Isidori and A. Retico, JHEP 0209 (2002) 063 [hep-ph/0208159].

[18] A. Dedes and A. Pilaftsis, Phys. Rev. **D67** (2003) 015012 [hep-ph/0209306].

[19] D. A. Demir, Phys. Lett. **B571**, 193 (2003) [hep-ph/0303249].

[20] S. Heinemeyer , W. Hollik, F. Merz and S. Peñaranda, Eur. Phys. J. **C37** (2004) 481 [hep-ph/0403228]; hep-ph/0506104.

[21] C. S. Huang, X. H. Wu and S. H. Zhu, Phys. Lett. **B452** (1999) 143 [hep-ph/9901369]; J. Phys. G **25** (1999) 2215 [hep-ph/9902474].

[22] F. Borzumati, C. Greub, T. Hurth and D. Wyler, Phys. Rev. **D62** (2000) 075005 [hep-ph/9911245]; T. Besmer, C. Greub and T. Hurth, Nucl. Phys. **B609** (2001) 359 [hep-ph/0105292].

[23] M. Ciuchini, E. Franco, A. Masiero and L. Silvestrini, Phys. Rev. **D67** (2003) 075016 [Erratum-ibid. **D68** (2003) 079901 [hep-ph/0212397]; M. Endo, M. Kakizaki and M. Yamaguchi, Phys. Lett. **B583** (2004) 186 [hep-ph/0311072].

[24] R. Mertig, M. Bohm and A. Denner, Comput. Phys. Commun. **64** (1991) 345; T. Hahn and C. Schappacher, Comput. Phys. Commun. **143** (2002) 54 [hep-ph/0105349]; T. Hahn, Comput. Phys. Commun. **140** (2001) 418 [hep-ph/0012260]; T. Hahn and M. Perez-Victoria, Comput. Phys. Commun. **118** (1999) 153 [hep-ph/9807565].
The codes are accessible via *www.feynarts.de*.

[25] S. Heinemeyer, W. Hollik and G. Weiglein, Comput. Phys. Commun. **124** (2000) 76 [hep-ph/9812320]; Eur. Phys. J. **C9** (1999) 343 [hep-ph/9812472]; hep-ph/0002213; M. Frank, S. Heinemeyer, W. Hollik and G. Weiglein, hep-ph/0202166; G. Degrassi,

S. Heinemeyer, W. Hollik, P. Slavich and G. Weiglein, Eur. Phys. J. **C**28 (2003) 133 [hep-ph/0212020].
The code is accessible via *www.feynhiggs.de*.

[26] M. Carena, D. Garcia, U. Nierste and C. E. M. Wagner, Nucl. Phys. **B577**, 88–120 (2000) [hep-ph/9912516]; J. Guasch, P. Häfliger and M. Spira, Phys. Rev. **D68**, 115001 (2003) [hep-ph/0305101].

[27] S. Dawson and L. Reina, Phys. Rev. **D60** (1999) 015003 [hep-ph/9812488]; Phys. Rev. **D59** (1999) 054012 [hep-ph/9808443].

[28] Particle Data Group, K. Hagiwara *et al.*, "Review of particle physics," Phys. Rev. **D66**, 010001 (2002).

[29] R. Barate *et al.* [ALEPH Collaboration], Phys. Lett. **B565** (2003) 61 [hep-ex/0306033].

[30] R. Barate *et al.* [ALEPH Collaboration], Phys. Lett. **B429** (1998) 169; S. Ahmed *et al.* [CLEO Collaboration], hep-ex/9908022.

[31] G. Belanger, F. Boudjema, A. Pukhov and A. Semenov, Comput. Phys. Commun. **149** (2002) 103 [hep-ph/0112278].

[32] V. D. Barger, M. S. Berger, P. Ohmann and R. J. Phillips, Phys. Rev. **D51** (1995) 2438 [hep-ph/9407273].

[33] G. Degrassi, P. Gambino and G. F. Giudice, JHEP **0012** (2000) 009 [hep-ph/0009337].

[34] H. E. Haber, M. J. Herrero, H. E. Logan, S. Peñaranda, S. Rigolin and D. Temes, Phys. Rev. **D63** (2001) 055004 [hep-ph/0007006]; hep-ph/0102169; M. J. Herrero, S. Peñaranda and D. Temes, Phys. Rev. **D64** (2001) 115003 [hep-ph/0105097]; H. E. Haber, H. E. Logan, S. Peñaranda and D. Temes, hep-ph/0601237.

[35] R. A. Jiménez and J. Solà, Phys. Lett. **B389**, 53 (1996) [hep-ph/9511292]; A. Bartl, H. Eberl, K. Hidaka, T. Kon, W. Majerotto and Y. Yamada, Phys. Lett. **B378**, 167 (1996) [hep-ph/9511385]; H. Eberl, K. Hidaka, S. Kraml, W. Majerotto and Y. Yamada, Phys. Rev. **D62** (2000) 055006 [hep-ph/9912463].

[36] A. Dobado, M. J. Herrero and D. Temes, Phys. Rev. **D65** 075023 (2002) [hep-ph/0107147]; A. M. Curiel, M. J. Herrero, D. Temes and J. F. de Troconiz, Phys. Rev. **D65** 075006 (2002) [hep-ph/0106267].

[37] J. Guasch, W. Hollik and S. Peñaranda, Phys. Lett. **B 515**, 367 (2001) [hep-ph/0106027]; hep-ph/0307012; M. Carena, H. E. Haber, H. E. Logan and S. Mrenna, Phys. Rev. **D65** (2002) 055005 [Erratum-ibid. D **65** (2002) 099902] [hep-ph/0106116].

[38] K. S. Babu and C. Kolda, Phys. Rev. Lett. **89** (2002) 241802 [hep-ph/0206310]; A. Dedes, J. R. Ellis and M. Raidal, Phys. Lett. **B549** (2002) 159 [hep-ph/0209207]; A. Brignole and A. Rossi, Phys. Lett. **B566**, 217 (2003) [hep-ph/0304081].